CHAPTER 6:
System Throughput and SNR / Exposure Time Estimation

In This Chapter...

6.1 System Throughput

A decision on a suitable exposure time will require the combination of

- The overall spectral response of the system (Figure 2.4).
- The spectral transmission of the filters (Chapter 3 and Appendix A).
- The spectral energy distribution and spatial profile of the target.
- The point response function and pixel size of the instrument (Chapter 5).
- Criteria for specifying desirable charge levels.

When the transmissions of filters $T(\lambda)$ are combined with the overall system response $Q(\lambda)$, we obtain detective quantum efficiency plots (electrons-per-photon as a function of λ) for each filter. These DQE plots link the output of the CCD to the photon flux at the input to an unobscured 2.4 m telescope.

These calibrations exist in the STScI Calibration Data Base, and are accessible with the STSDAS SYNPHOT package or with the XCAL software. The XCAL and SYNPHOT Users Guides should be consulted for further details. We include here a sufficient calibration for exposure planning.

In Table 6.1 the dimensionless efficiency and the mean wavelength for each filter are tabulated together with the effective width, the equivalent Gaussian dimensionless width, the maximum transmission, the derivative of the mean wavelength with respect to spectral index, the pivot wavelength, average wavelength, and wavelength of maximum transmission. The parameters are defined as follows. The dimensionless efficiency is

$$\int Q(\lambda)T(\lambda)d\lambda/\lambda$$

The mean wavelength is defined in Schneider, Gunn, and Hoessel Ap. J., 264, 337 (1983)

$$\bar{\lambda} = \exp\left[\frac{\int Q(\lambda)T(\lambda)\log_e(\lambda)d\lambda/\lambda}{\int Q(\lambda)T(\lambda)d\lambda/\lambda}\right]$$

This rather unconventional definition has the property that the correspondingly defined mean frequency is just $c/\bar{\lambda}$. It is in some sense halfway between the conventional frequency mean and the wavelength mean. The pivot wavelength is defined as

$$\lambda_p = \left[\frac{\int Q(\lambda)T(\lambda)\lambda d\lambda}{\int Q(\lambda)T(\lambda)d\lambda/\lambda}\right]^{1/2}$$

The effective dimensionless Gaussian width is defined implicitly by

$$\sigma^2 = \left[\frac{\int_{\bar{\lambda}(1-5\sigma)}^{\bar{\lambda}(1+5\sigma)} Q(\lambda)T(\lambda)\left[\log_e\left(\frac{\lambda}{\bar{\lambda}}\right)\right]^2\frac{d\lambda}{\lambda}}{\int_{\bar{\lambda}(1-5\sigma)}^{\bar{\lambda}(1+5\sigma)} Q(\lambda)T(\lambda)\frac{d\lambda}{\lambda}}\right]$$

where the integration limits eliminate unrealistic contributions from imperfect blocking far from the bandpass. The effective width of the bandpass is

$$\delta\bar{\lambda} = 2[2\log_e 2]^{1/2}\sigma\bar{\lambda}$$

The final two columns in Table 6.1 are defined as follows. In the next-to-last column $m_{e/sec}$ is the zero-point magnitude for 1 e^- s^{-1} (with AB_ν=0). The final column gives t_{wfsky}, which is the exposure time (in seconds) needed to make the sky noise equal to 5 e^- RMS (i.e. ~read noise) in the WFC for a sky level of V=23.3 mag arcsec^{-2}.

Table 6.1: System Efficiencies and Zeropoints. See Section 6.1 for definitions. [a]

Filter	$\int QTd\lambda/\lambda$	$\bar{\lambda}$	$\delta\bar{\lambda}$	σ	QT_{max}	$d\bar{\lambda}/d\alpha$	λ_p	$<\lambda>$	λ_{max}	$m_{e/sec}$	t_{wfsky}
F122M	0.00012	1419.7	438.2	0.1311	0.00118	24.40	1748.5	2018.0	1258	18.69	1.7E+06
F130LP	0.09178	5115.8	4776.0	0.3965	0.12977	804.10	5786.6	6107.1	6386	25.90	
F160AW	0.00021	1491.8	448.9	0.1278	0.00065	24.36	1517.3	1530.4	1406	19.30	9.5E+05
F160BW	0.00021	1491.8	448.9	0.1278	0.00065	24.36	1517.3	1530.4	1406	19.30	9.5E+05
F165LP	0.08841	5195.6	4541.2	0.3712	0.12633	715.80	5817.0	6118.8	6386	25.86	
F170W	0.00057	1749.8	545.5	0.1324	0.00178	30.67	1824.6	1872.6	1834	20.38	3.5E+05
F185W	0.00035	1952.9	335.0	0.0729	0.00188	10.37	1971.9	1983.1	1936	19.86	9.1E+06
F218W	0.00057	2191.6	387.9	0.0752	0.00275	12.38	2205.2	2212.2	2248	20.38	5.6E+06
F255W	0.00078	2585.8	393.2	0.0646	0.00452	10.78	2597.3	2603.1	2546	20.73	4.1E+06
F300W	0.00519	2942.8	735.8	0.1062	0.01838	33.17	2981.9	3002.7	2866	22.78	7.1E+04
F336W	0.00403	3342.2	381.1	0.0484	0.02872	7.84	3359.4	3369.2	3456	22.51	3.3E+04
F343N	0.00006	3432.9	27.3	0.0034	0.00691	0.04	3440.4	3445.6	3432	17.94	2.2E+06
F375N	0.00006	3737.5	27.3	0.0031	0.00774	0.04	3743.0	3746.7	3737	17.94	9.0E+05
F380W	0.00693	3964.4	673.0	0.0721	0.03406	20.61	3984.8	3995.0	3994	23.10	7.8E+03
F390N	0.00029	3888.7	45.2	0.0049	0.01880	0.10	3889.6	3890.3	3885	19.65	1.9E+05
F410M	0.00164	4090.1	146.7	0.0152	0.03619	0.95	4092.6	4093.9	4098	21.53	3.3E+04
F437N	0.00019	4370.3	25.3	0.0025	0.02681	0.03	4369.6	4369.7	4368	19.19	1.8E+05
F439W	0.00501	4299.8	473.3	0.0467	0.03436	9.40	4309.6	4314.4	4186	22.74	6.9E+03
F450W	0.01501	4519.1	956.6	0.0899	0.07955	36.52	4555.1	4572.9	5066	23.94	2.3E+03
F467M	0.00216	4668.7	166.7	0.0152	0.04825	1.07	4669.9	4670.5	4732	21.83	1.6E+04
F469N	0.00023	4694.4	24.9	0.0022	0.03267	0.02	4694.5	4694.5	4699	19.40	1.5E+05
F487N	0.00029	4865.1	25.8	0.0023	0.04239	0.03	4865.4	4865.8	4866	19.65	8.5E+04
F502N	0.00037	5012.2	26.8	0.0023	0.05226	0.03	5013.1	5013.1	5008	19.92	6.7E+04
F547M	0.01224	5476.3	483.1	0.0375	0.10577	7.69	5484.0	5487.8	5566	23.71	2.0E+03
F555W	0.02727	5397.5	1226.4	0.0965	0.10312	50.26	5447.9	5473.3	5536	24.58	9.0E+02
F569W	0.02139	5614.2	965.7	0.0730	0.10587	29.96	5644.9	5660.3	5536	24.32	8.8E+02
F588N	0.00133	5893.5	49.0	0.0035	0.12054	0.07	5893.5	5893.6	5894	21.30	1.4E+04
F606W	0.04191	5935.0	1497.3	0.1071	0.13468	68.12	6002.3	6036.1	6194	25.05	4.5E+02
F622W	0.02649	6162.8	916.5	0.0632	0.13123	24.58	6187.5	6199.8	6416	24.55	7.1E+02
F631N	0.00078	6306.4	30.8	0.0021	0.11709	0.03	6306.4	6306.4	6306	20.73	2.4E+04
F656N	0.00045	6563.7	21.4	0.0014	0.10379	0.01	6563.7	6564.0	6561	20.13	3.4E+04
F658N	0.00063	6590.1	28.5	0.0018	0.10574	0.02	6590.8	6590.9	6596	20.49	2.4E+04
F673N	0.00104	6732.1	47.2	0.0030	0.11134	0.06	6732.2	6732.3	6736	21.04	1.5E+04
F675W	0.02169	6695.9	865.6	0.0549	0.12770	20.18	6716.1	6726.2	6634	24.34	7.1E+02
F702W	0.03206	6867.8	1382.5	0.0855	0.13397	50.19	6918.8	6944.5	6514	24.76	4.8E+02
F785LP	0.00780	8617.0	1331.7	0.0656	0.04378	37.11	8654.8	8673.9	8306	23.23	1.6E+03
F791W	0.01589	7826.3	1205.0	0.0654	0.09120	33.46	7860.5	7877.7	7364	24.00	7.9E+02
F814W	0.01799	7920.9	1488.8	0.0798	0.09937	50.47	7973.0	7999.5	7266	24.13	7.0E+02
F850LP	0.00395	9072.1	985.8	0.0461	0.03491	19.32	9091.6	9101.6	8800	22.49	2.9E+03
F953N	0.00012	9544.7	52.5	0.0023	0.01651	0.05	9544.7	9544.8	9526	18.69	9.6E+04
F1042M	0.00012	10183.5	365.0	0.0152	0.00359	2.36	10188.8	10191.1	10110	18.69	8.7E+04
FQUVN-A	0.00028	3765.4	73.1	0.0082	0.01122	0.26	3766.0	3766.6	3803	19.61	4.7E+05
FQUVN-B	0.00028	3830.2	57.1	0.0063	0.01465	0.15	3830.7	3831.3	3827	19.61	1.9E+05
FQUVN-C	0.00038	3912.9	59.3	0.0064	0.01949	0.16	3914.4	3915.0	3907	19.94	1.4E+05
FQUVN-D	0.00045	3992.3	63.5	0.0068	0.02244	0.18	3992.9	3993.2	3992	20.13	1.2E+05
FQCH4N-A	0.00075	~5433	~38	0.0028	0.09356	0.04	-	-	5443	20.68	3.3E+04
FQCH4N-B	0.00082	~6193	~44	0.0028	0.11360	0.05	-	-	6205	20.78	2.3E+04
FQCH4N-C	0.00062	~7274	~51	0.0024	0.09075	0.04	-	-	7279	20.48	2.5E+04
FQCH4N-D	0.00026	~8929	~64	0.0067	0.03334	0.39	-	-	8930	19.53	4.4E+04
POLQ_par	0.06005	5570.9	4184.5	0.3190	0.09298	566.81	6076.2	6323.3	6476	25.44	
POLQ_per	0.01299	7027.7	5153.2	0.3114	0.03744	681.43	7541.1	7766.0	7839	23.78	

a. It is anticipated the values for filters F160BW and FQCH4N will be updated in mid-1996.

Table 6.2: AB_ν as a Function of Wavelength. AB_ν is defined as a color-dependent correction from V magnitude to AB magnitude at frequency ν. Wavelength (Å) runs along the top; spectral classes run down the leftmost column. The second column contains B-V. See Section 6.3.

	B-V	1500	2000	2500	3000	3500	4000	4500	5000	6000	7000	8000	9000	10000
sky	1.10	2.45	5.46	5.46	3.12	2.00	1.03	0.55	0.18	-0.11	-0.33	-0.55	-0.65	-0.75
B0	-0.31	-1.60	-1.50	-1.20	-0.78	-0.62	-0.46	-0.36	-0.22	0.16	0.46	0.76	0.96	1.17
A0	0.00	2.22	1.35	1.11	1.21	1.00	-0.23	-0.16	-0.09	0.11	0.22	0.33	0.36	0.4
F0	0.27	7.22	4.10	3.11	1.99	1.38	0.29	0.06	0.03	0.03	0.05	0.08	0.09	0.1
G0	0.58	8.9	6.35	4.61	2.46	1.63	0.67	0.26	0.08	-0.04	-0.12	-0.21	-0.23	-0.25
K0III	1.07	13	10.3	8.11	5.46	2.13	1.16	0.46	0.2	-0.24	-0.42	-0.61	-0.66	-0.72
M0III	1.60	15	12.3	9.36	6.21	4.63	2.26	0.96	0.51	-0.46	-0.76	-1.06	-1.12	-1.19
gE	1.00	6.82	6.41	5.43	3.63	2.49	1.40	0.55	0.21	-0.19	-0.52	-0.81	-1.07	-1.29
Sa	0.80	5.40	4.80	4.10	3.00	2.01	1.12	0.44	0.19	-0.17	-0.44	-0.7	-0.95	-1.16
Sbc	0.60	4.03	3.18	2.86	2.46	1.54	0.84	0.34	0.17	-0.14	-0.37	-0.6	-0.84	-1.04
Scd	0.45	2.67	2.29	2.15	1.76	1.35	0.65	0.28	0.13	-0.11	-0.26	-0.39	-0.47	-0.58
Ir I	0.30	1.77	1.40	1.36	1.24	0.94	0.43	0.34	0.17	0.13	-0.04	-0.21	-0.33	-0.45

6.2 On-Line Exposure Time Calculator

We note that most of the calculations below are incorporated in the on-line WFPC2 Exposure Time Calculator (ETC) program, which is available on the WFPC2 WWW pages at

`http://www.stsci.edu/ftp/instrument_news/WFPC2/wfpc2_top.html`

on the software tools page.

To use this program, one merely fills out an “HTML” form giving the target information (e.g. magnitude and color), camera configuration (PC or WFC, desired gain setting, and filter), and either the exposure time or the desired signal-to-noise ratio. As of this writing there are separate HTML forms for point sources, extended sources, point source with background light, and extended targets with background light. After filling out the form the user then clicks on “calculate” and the program returns the resulting signal-to-noise ratio if the exposure time was specified, or vice versa. Examples of completed HTML forms and results are shown in “Sample SNR Calculations” on page 123. Note that clicking on any colored text on the HTML form will give a description of that item.

The ETC program handles sources with stellar spectra, power law sources, and emission line sources; point sources and extended sources; and sources superposed on a diffuse stellar background. The program also returns advice on CR-SPLITing, use of CLOCKS=YES, and warnings about saturation, if appropriate. The program currently (Version 2.0) assumes stellar data will be analyzed by PSF fitting. Results are typically accurate to a few percent.

While observers should familiarize themselves with the material below, most will find the ETC program faster and easier to use for actual calculations. The ETC program will also be updated to reflect any changes in instrument performance, so observers can be assured of up-to-the-minute information.

6.3 Target Count Rates

We now consider estimation of count rates for objects with stellar, power law, and emission line spectra.

6.3.1 Count Rates for Stellar Sources

To estimate the number of electrons collected from a point source of apparent visual magnitude V, one can use the equation:

$$N = 2.5 \times 10^{11} \cdot t \cdot [\int Q(\lambda) T(\lambda) d\lambda / \lambda] \times 10^{-0.4(V + AB_\nu)} \qquad (6.1)$$

where t is the exposure time in seconds, the QT integral is given in Table 6.1, and AB_ν is given in Table 6.2 as a function of spectral type and wavelength for some example spectral energy distributions. The quantity AB_ν is a color-dependent correction from V magnitude to AB magnitude at frequency ν. The AB magnitude system is defined as (Oke and Gunn 1983)

$$AB = V + AB_\nu = -2.5 \cdot \log F_\nu - 48.60$$

where F_ν is the flux in erg cm^{-2} s^{-1} Hz^{-1}.

Equation 6.1 may be trivially rewritten to give the count rate R_{object} in units of e$^-$ s^{-1} pixel^{-1} for a target with a stellar spectrum as:

$$R_{object} = 2.5 \times 10^{11} \cdot [\int Q(\lambda) T(\lambda) d\lambda / \lambda] \cdot 10^{-0.4(V + AB_\nu)} \qquad (6.2)$$

6.3.2 Count Rates for Power Law Sources

If one knows the spectral index α (which is zero for a source with a flat continuum), $V+AB_\nu$ can also be calculated as the monochromatic Oke system magnitude at the corrected mean wavelength of the filter:

$$V + AB_\nu = -2.5\log_{10}(S_\nu[\bar{\lambda} + \alpha(d\bar{\lambda}/d\alpha)]) - 48.6$$

where S_ν is the flux in ergs cm^{-2} s^{-1} Hz^{-1} as in Oke and Gunn, Ap. J., 266, 713 (1983) at the effective mean wavelength of the filter $\bar{\lambda} + \alpha(d\bar{\lambda}/d\alpha)$. It can be shown that

$$\frac{d\bar{\lambda}}{d\alpha} = \bar{\lambda}\sigma^2$$

if the integrands are weighted by a source with spectral index α in the definition of λ. See also Koornneef, J., et al. "Synthetic Photometry and the Calibration of the Hubble Space Telescope" in Highlights of Astronomy (7, 833, J.-P. Swings Ed (1983). Combining the above equations gives

$$R_{object} = 6.9 \times 10^{30} \cdot [\int Q(\lambda)T(\lambda)d\lambda/\lambda] \cdot S_\nu\left(\bar{\lambda} + \alpha\frac{d\bar{\lambda}}{d\alpha}\right) \qquad (6.3)$$

6.3.3 Count Rates for Emission Line Sources

The count rate in units of e^- s^{-1} for a monochromatic emission line is given by

$$R_{object} = 2.3 \times 10^{12} \cdot (QT) \cdot F \cdot \lambda \qquad (6.4)$$

where F is the emission line flux in units of ergs cm^{-2} s^{-1}, and λ is the wavelength of the line in Angstroms. The quantity QT is the (system + filter) quantum efficiency at the wavelength of the line, which can be determined from inspection of the figures in section A.2, "Passbands including the System Response", on page 211. For lines near the maxima of the filter transmission curves, it should be sufficient to use QT_{max} from Table 6.1. Note that the integrated filter efficiency is not relevant for the signal calculation.

In cases where the width of the line approaches that of the filter, it will be necessary to convolve the line shape and filter bandpass using either the SYNPHOT or XCAL programs.

For example, H_α emission at 6563Å, with total source flux F=10^{-16} erg s^{-1} cm^{-2}, observed through the F656N filter (total system throughput T=0.104 from "F656N, F658N, F673N, F675W, F702W, F785LP" on page 217), will produce a target count rate R_{object}=0.155 e^- s^{-1} integrated over the entire source.

6.4 Sky Background

The sky background can contribute significant Poisson noise in broad and medium band filters, and must be taken into account during noise calculations. The actual sky brightness depends on the heliocentric ecliptic coordinates (latitude and longitude) in a manner summarized in Table 6.3. The appropriate AB_V can be taken from Table 6.2. To convert mag arcsec^{-2} to mag pixel^{-1} one needs to add 5 magnitudes (WFC) or 6.7 magnitudes (PC1). These values are actually lower limits on the effective sky-brightness that will be seen, because light from the bright Earth limb can scatter into the aperture.

If your observations are sky background limited, and signal-to-noise is a driver, consider the use of the special requirement LOW-SKY as described in the *Call for Proposals* or the *Phase II Proposal Instructions*. LOW-SKY has two effects:

- It causes the observation to be scheduled at the time of year when the zodiacal background light is within 30% of the minimum possible background value for the target, and
- It requires that the observation be made when the bright Earth limb is more than 40˚ from the OTA axis, which greatly reduces scattered light.

For many targets LOW-SKY will have minimal impact on the observing efficiency. Note, however, that targets in the Continuous Viewing Zone (CVZ) cannot be observed if LOW-SKY is specified. See “Observing Faint Targets” on page 143 for more information.

Table 6.3: Sky Brightness (V mag arcsec^{-2}) as a Function of Heliocentric Ecliptic Latitude and Longitude. “SA” denotes that the target is unobservable due to solar avoidance.

Heliocentric Ecliptic Longitude	Ecliptic Latitude						
	0˚	15˚	30˚	45˚	60˚	75˚	90˚
180˚	22.1	22.4	22.7	23.0	23.2	23.4	23.3
165˚	22.3	22.5	22.8	23.0	23.2	23.4	23.3
150˚	22.4	22.6	22.9	23.1	23.3	23.4	23.3
135˚	22.4	22.6	22.9	23.2	23.3	23.4	23.3
120˚	22.4	22.6	22.9	23.2	23.3	23.3	23.3
105˚	22.2	22.5	22.9	23.1	23.3	23.3	23.3
90˚	22.0	22.3	22.7	23.0	23.2	23.3	23.3
75˚	21.7	22.2	22.6	22.9	23.1	23.2	23.3
60˚	21.3	21.9	22.4	22.7	23.0	23.2	23.3
45˚	SA	SA	22.1	22.5	22.9	23.1	23.3
30˚	SA	SA	SA	22.3	22.7	23.1	23.3
15˚	SA	SA	SA	SA	22.6	23.0	23.3
0˚	SA	SA	SA	SA	22.6	23.0	23.3

Another option for reducing the sky brightness, is the special requirement SHADOW, which forces the observation to be made when HST is in the Earth's shadow. This usually has a large negative impact on the observing efficiency, and is recommended only when attempting to avoid geocoronal lines when observing far-UV emission lines (e.g. Ly α and OI 1304Å). Moreover, it does not attempt to minimize zodiacal emission, which dominates at visible wavelengths.

Table 6.4 shows approximate sky count rates for the WFC and PC1 for filters with significant sky count rates. An average sky brightness of V=22.9 mag arcsec^{-2} is assumed. Filters not listed in the table have sky count rates below that of the dark current, so the sky contribution will generally be unimportant. Values for other filters or sky brightnesses can be computed from Table 6.2, Table 6.1, Table 6.3, and Equation 6.2.

Table 6.4: Sky Count Rate per Pixel (P_{sky}). An average sky brightness of V = 22.9 mag arcsec^{-2} is assumed. Filters not listed have sky rate significantly below the dark current.

Filter	Sky Count Rate (P_{sky}) (e^{-} s^{-1} $pixel^{-1}$)	
	WFC	PC1
F336W	0.0009	0.0002
F380W	0.005	0.001
F439W	0.005	0.0011
F450W	0.018	0.004
F467M	0.003	0.0006
F547M	0.021	0.0045
F555W	0.052	0.010
F588N	0.002	0.0006
F569W	0.040	0.0081
F606W	0.090	0.020
F622W	0.060	0.012
F673N	0.002	0.0006
F675W	0.056	0.012
F702W	0.082	0.0016
F785LP	0.024	0.0050
F791W	0.048	0.010
F814W	0.054	0.011
F850LP	0.012	0.0024

6.5 Signal-to-Noise Ratio Estimation

The signal-to-noise ratio (SNR) for a point source depends on both the Poisson noise of the object, and on noises associated with the background. Sources of background noise include “read noise” of the CCDs, and Poisson noise in the dark current, sky background, and any smooth galaxy light superposed on the target.

The SNR obtained for photometry of a point source will depend on the analysis technique used. The optimum SNR will be obtained when the pixels of the point source PSF are weighted in proportion to their expected intensity by PSF fitting. Aperture photometry will tend to give lower SNR, especially for sources where the background is important, but nonetheless is widely used. We now consider both methods.

6.5.1 Point Sources -- PSF Fitting

In the bright target limit, Poisson noise sets the SNR and

$$SNR = (S)^{1/2} = (R_{object} \cdot t)^{1/2}$$

where S is the number of detected photons, and R_{object} is given by the above equations 6.2 through 6.4, and t is the exposure time.

In the background limited case (e.g. read noise, dark current, or sky noise limited) the SNR is a function not only of the expected number of detected photons S from the source but also of the average effective background count rate in each pixel B, the point spread function $(PSF)_{i,\,j}$, and the weights used to average the signal in the pixels affected by the source. It is easy to show that the signal-to-noise ratio for optimal weights (which are proportional to the point spread function) is given by:

$$SNR = \frac{S}{\sqrt{B}} \cdot \left(\sum (PSF)_{i,\,j}{}^{2}\right)^{1/2} = \frac{S}{\sqrt{B}} \cdot (sharpness)^{1/2} \qquad (6.5)$$

Where *sharpness* is effectively the reciprocal of the number of pixels contributing background noise. The summation is tabulated for a few representative cases in Table 6.5. To estimate the signal-to-noise, multiply the signal-to-noise obtained, assuming all the flux is in one pixel, by the square root of the value in the Table.

Table 6.5: Sharpness as a Function of Wavelength, Camera, and Location of the Star Center with Respect to the Pixel Grid. The "Obs." columns represent the values for the real OTA, WFPC2 optics, and CCD MTF function. The "Diff." column represents values for the theoretical diffraction limit with perfect optics and detectors. Target location refers to both the camera used (PC or WFC), and the location of the star center on the pixel grid.

Target Location	2000 Å		4000 Å		6000 Å		8000 Å	
	Obs.	Diff.	Obs.	Diff.	Obs.	Diff.	Obs.	Diff.
PC Pixel Center	0.084	0.409	0.095	0.259	0.066	0.115	0.046	0.073
PC Pixel Corner	0.063	0. 186	0.065	0.107	0.054	0.072	0.045	0.068
WFC Pixel Center	0.120	0.745	0.145	0.482	0.128	0.318	0.124	0.285
WFC Pixel Corner	0.102	0.228	0.105	0.193	0.098	0.178	0.081	0.126

We note that PSF fitting is equivalent to convolving the image with the PSF, and then measuring the peak counts for stellar objects. Also, the location of the star on the pixel grid will be impossible to know in advance of the observation (i.e. pixel center vs. pixel corner in Table 6.5). In general, the lower "pixel corner" values should be used, so as to insure adequate SNR.

The average effective background counts per exposure and per pixel can be expanded to include various sources:

$$B = readnoise^2 + P_{dark} \cdot (t + 46) + P_{sky} \cdot t + P_{background} \cdot t$$

where terms include the read out noise of the CCD (*readnoise*), the dark current (P_{dark}), sky background count rate (P_{sky}), and the count rate of any diffuse background light from astrophysical sources ($P_{background}$). Herein we will use "*P*" to represent count rates **per pixel**, and "*R*" to represent the **total** counts for an object. The exposure time is represented by *t*.

For example, Table 2.2 lists the faintest V magnitude star, V=28.14, measurable with a signal-to-noise ratio of 3 in a 3000s integration in F569W in the Wide Field Cameras. The calculation to check this goes as follows. The efficiency of the filter is 0.02139 from Table 6.1. The sky background in each pixel is 23.3+5=28.3, assuming an ecliptic latitude of 90° from Table 6.3, and the pixel area correction for the WFC given in that section. The total sky background collected per pixel in 3000 seconds is given by Equation 6.1 as 76.8 electrons. Note that the AB_ν color correction required for the sky in the wavelength range of the filter is 0.0 from Table 6.2. From Table 4.3, the read noise is 5.2 electrons. From Table 4.2, the median dark current at -88 ˚C is 0.004. Therefore the total dark current (on which there will be shot noise) is only 12 electrons. The equivalent background per pixel is then given as B=76.8+5.2^2+12=116. The total number of detected electrons from a star with V=28.14 is S=89 electrons, again using Equation 6.1. The expected peak count is 27 detected electrons using Table

5.4, which is much less than B, requiring the use of Equation 6.5 for the background limited case. The sharpness for the WF camera in the best case, when the star is centered on a pixel, is given in Table 6.5 as 0.128. Then Equation 6.5 above gives the signal-to-noise as 3.0:

$$SNR = \left(\frac{89}{\sqrt{116}} \cdot \sqrt{0.128}\right) = 3.0$$

If, instead, the peak count rate comes out much greater than the background, the observation is photon noise limited, and the signal-to-noise should be computed as the square root of the signal S in electrons.

In principle, one should also include contributions in the signal-to-noise for flat fielding uncertainties, noise in the bias and dark calibration files, and quantization noise. Flat fielding errors will be of order 1%, and will limit SNR in the large-signal limit. Noise in the bias and dark calibration files will be unimportant in most pixels, although these could become important if many (>10) non-dithered frames of the same field are combined.

Quantization noise can be estimated as $gain/\sqrt{12}$ (i.e., $\sqrt{4.1}$ in the 7 $e^- DN^{-1}$ channel, and $\sqrt{16.3}$ in the 14 $e^- DN^{-1}$ channel). In nearly all situations it can be ignored. In the weak signal case, the quantization noise is effectively included in the read noise values given throughout this Handbook; in the strong signal case it is very small compared to the Poisson noise and can be ignored.

A generalized equation for estimating point source signal-to-noise ratio per exposure is given below (Equation 6.6). It is exact in both the bright and faint object limits, and is a reasonable approximation to the intermediate case. $P_{background}$ represents any generalized source of diffuse background light (e.g. galaxy on which target is superposed). Table 6.6 gives rough values for some of the parameters, along with references for more accurate values.

$$SNR = \frac{R_{object} \cdot t}{\sqrt{R_{object} \cdot t + \frac{readnoise^2 + P_{dark} \cdot (t + 46) + P_{sky} \cdot t + P_{background} \cdot t}{sharpness}}} \quad (6.6)$$

Note that in this formulation, $sharpness^{-1}$ is the equivalent number of pixels the weighted signal is integrated over. In the event that multiple exposures are taken (e.g. to remove cosmic rays), the signal-to-noise ratio for the final averaged image is approximately given by:

$$SNR_{total} = SNR \cdot \sqrt{N}$$

where N is the number of images averaged.

Table 6.6: Parameters for Point Source SNR Estimation - PSF Fitting

Parameter	Description	Units	Approx. Value	Better Value
R_{object}	object count rate	$e^{-}\ s^{-1}$		Equation 6.1, 6.2, or 6.3
P_{dark}	dark count rate	$e^{-}\ s^{-1}\ pixel^{-1}$	0.004	Table 4.2
P_{sky}	sky count rate	$e^{-}\ s^{-1}\ pixel^{-1}$	Table 6.4	Tables 6.2, 6.1, 6.3; Eqn 6.1
$P_{background}$	count rate from background light (if any)	$e^{-}\ s^{-1}\ pixel^{-1}$		Tables 6.2, 6.1; Eqn 6.1
read noise		e^{-}	ATD-GAIN=7 use 5.3[a] ATD-GAIN=15 use 7.5	Table 4.3
sharpness			WFC use 0.11 PC1 use 0.06	Table 6.5
t	exposure time	s		

a. ATD-GAIN defaults to 7 unless otherwise specified on Phase 2 proposal.

6.5.2 Point Sources -- Aperture Photometry

When aperture photometry is used, one must consider the fraction of the object counts encircled by the aperture, as well the background noise in the aperture. In the bright target limit the SNR is given by

$$SNR = (S \cdot f(r))^{1/2} = (R_{object} \cdot f(r) \cdot t)^{1/2}$$

where S is the number of detected photons, $f(r)$ is the fraction of the total counts encircled by the aperture with radius r, and R_{object} is target count rate. Representative values of $f(r)$ are given in Table 6.7; values for other aperture sizes and filters can be estimated from Figure 5.3 on page 88, or Figure 5.4 on page 89.

In the faint target limit the noise contributed by background counts determines the SNR

$$SNR = \frac{S \cdot f(r)}{\sqrt{B \cdot \pi r^2}}$$

where B represents the effective background counts per pixel, and r is the aperture radius in pixels.

In the generalized case the SNR per exposure for aperture photometry is given approximately by:

$$SNR = \frac{f(r) \cdot R_{object} \cdot t}{\sqrt{(f(r) \cdot R_{object} \cdot t) + [readnoise^2 + P_{dark} \cdot (t + 46) + P_{sky} \cdot t + P_{background} \cdot t] \cdot \pi r^2}} \qquad (6.7)$$

where the parameters are summarized in Table 6.8.

Table 6.7: Encircled Energy for Representative Filters. Encircled energy values are normalized to unity at large radius.

CCD	Aperture Radius (r)	Encircled Energy f(r)		
		F218W	F555W	F814W
PC1	0.1″	0.60	0.67	0.53
	0.2″	0.73	0.85	0.78
	0.5″	0.84	0.96	0.87
	1.0″	0.92	1.00	0.92
WF3	0.1″	0.40	0.46	0.44
	0.2″	0.69	0.76	0.74
	0.5″	0.85	0.90	0.91
	1.0″	0.94	0.94	0.96

Table 6.8: Parameters for Point Source SNR Estimation - Aperture Photometry.

Parameter	Description	Units	Approx. Value	Better Value
R_{object}	object count rate	$e^- s^{-1}$		Equation 6.1, 6.2, or 6.3
P_{dark}	dark count rate	$e^- s^{-1}$ pixel^{-1}	0.004	Table 4.2
P_{sky}	sky count rate	$e^- s^{-1}$ pixel^{-1}	Table 6.4	Tables 6.2, 6.1, 6.3; Eqn 6.1
$P_{background}$	count rate from back-ground light (if any)	$e^- s^{-1}$ pixel^{-1}		Tables 6.2, 6.1; Eqn 6.1
readnoise		e^-	ATD-GAIN=7 use 5.3[a] ATD-GAIN=15 use 7.5	Table 4.3
$f(r)$	encircled energy		Table 6.7	Figure 5.3 or 5.4
r	aperture radius	pixels		
t	exposure time	s		

a. ATD-GAIN defaults to 7 unless otherwise specified on Phase 2 proposal.

6.5.3 Extended Sources

The calculations for extended sources are nearly identical to those for point sources. The easiest procedure is to compute the SNR per detector pixel, and then adjust this value if the total SNR is required for an area encompassing many pixels.

In general, one will have the target magnitude or flux per square arcsecond. To compute the flux per pixel for the PC one merely multiplies the flux per square arcsecond by 0.00207, or instead, adds the value 6.7 to the magnitude per square arcsecond to get the necessary magnitude per PC pixel. For the WFC, one either multiplies the flux per square arcsecond by 0.00993, or adds 5.0 to the magnitude per square arcsecond. Equations 6.2, 6.3, and 6.4 can be rewritten including these factors as below.

PC Camera

For the PC camera, sources with stellar spectra, and V surface brightness per square arcsecond σ_V we have a count rate in e^- s^{-1} $pixel^{-1}$ of

$$P_{object} = 2.5 \times 10^{11} \cdot [\int Q(\lambda)T(\lambda)d\lambda/\lambda] \cdot 10^{-0.4(\sigma_V + AB_\nu + 6.7)} \quad (6.8)$$

For power law sources where B_ν is the target flux in units of ergs cm^{-2} s^{-1} Hz^{-1} $arcsec^{-2}$ we have

$$P_{object} = 1.4 \times 10^{28} \cdot [\int Q(\lambda)T(\lambda)d\lambda/\lambda] \cdot B_\nu\left(\bar{\lambda} + \alpha\frac{d\bar{\lambda}}{d\alpha}\right) \quad (6.9)$$

And finally for emission line sources where I_ν is the flux in ergs cm^{-2} s^{-1} $arcsec^{-2}$ we have

$$P_{object} = 4.8 \times 10^{9} \cdot (QT) \cdot I_\nu \cdot \lambda \quad (6.10)$$

where the emission line wavelength λ is in Angstroms.

WFC Camera

For the WFC camera and stellar sources with V surface brightness per square arcsecond σ_V we have a count rate in e^- s^{-1} $pixel^{-1}$ of

$$P_{object} = 2.5 \times 10^{11} \cdot [\int Q(\lambda)T(\lambda)d\lambda/\lambda] \cdot 10^{-0.4(\sigma_V + AB_\nu + 5)} \quad (6.11)$$

For power law sources where B_ν is the target flux in units of ergs cm^{-2} s^{-1} Hz^{-1} $arcsec^{-2}$ we have

$$P_{object} = 6.9 \times 10^{28} \cdot [\int Q(\lambda)T(\lambda)d\lambda/\lambda] \cdot B_\nu\left(\bar{\lambda} + \alpha\frac{d\bar{\lambda}}{d\alpha}\right) \quad (6.12)$$

And finally for emission line sources where I_ν is the flux in ergs cm^{-2} s^{-1} $arcsec^{-2}$ we have

$$P_{object} = 2.3 \times 10^{10} \cdot (QT) \cdot I_\nu \cdot \lambda \quad (6.13)$$

where the emission line wavelength λ is in Angstroms.

SNR

The generalized SNR per pixel per exposure for an extended source is then obtained simply by setting the sharpness to unity in equation 6.5:

$$SNR = \frac{P_{object} \cdot t}{\sqrt{P_{object} \cdot t + (readnoise^2 + P_{dark} \cdot (t + 46) + P_{sky} \cdot t + P_{background} \cdot t)}} \quad (6.14)$$

Table 6.9: Parameters for Extended Source SNR Estimation.

Parameter	Description	Units	Approx. Value	Better Value
P_{object}	object count rate	$e^{-}\ s^{-1}\ pixel^{-1}$		Equations 6.9 to 6.12
P_{dark}	dark count rate	$e^{-}\ s^{-1}\ pixel^{-1}$	0.004	Table 4.2
P_{sky}	sky count rate	$e^{-}\ s^{-1}\ pixel^{-1}$	Table 6.4	Tables 6.2, 6.1, 6.3; Eqn 6.7 (PC) or 6.10 (WFC)
$P_{background}$	count rate from background light (if any)	$e^{-}\ s^{-1}\ pixel^{-1}$		Tables 6.2, 6.1; Eqn 6.7 (PC) or 6.10 (WFC)
readnoise		e^{-}	ATD-GAIN=7 use 5.3[a] ATD-GAIN=15 use 7.5	Table 4.3
t	exposure time	s		

a. Default value is ATD-GAIN=7.

Since many observations of extended sources are for galaxies in broad-band filters, a few rules of thumb can be useful. Saturation is seldom a concern, except in very bright spots such as the inner core of ellipticals and of some bulges. Count rates for spiral galaxies range typically from 2 to 0.01 e^{-} $pixel^{-1}$ s^{-1} (and lower) for filters such as F555W, F606W, F702W, and F814W; the lower end of the range corresponds roughly to the de Vaucouleurs D_{25}. Count rates are significantly lower in blue and UV filters. Spiral structure can typically be traced reasonably well with total exposures of 3000 seconds or longer in the above filters.

For galaxies of very small angular size at red-shifts of cosmological interest, the image may cover a small number of pixels; thus the detection of such objects follows rules similar to those of point sources. However, the fraction of light falling in the central pixel is smaller for most galaxies than it is for true point sources. The approximate magnitude difference between the light falling in the central pixel and the entire galaxy is plotted in Figure 6.1 for a typical giant elliptical galaxy, as a function of redshift. For other types of galaxies, a morphological term can be added to the values (for example, 0.6 magnitudes for lenticulars, 0.7 for S, 0.8 for Sab, 0.9 for Sbc, 1.2 for Scd, and 1.8 for Irr). These values must be increased by an additional 1.7 magnitudes for the PC.

Figure 6.1: Giant Elliptical Galaxy

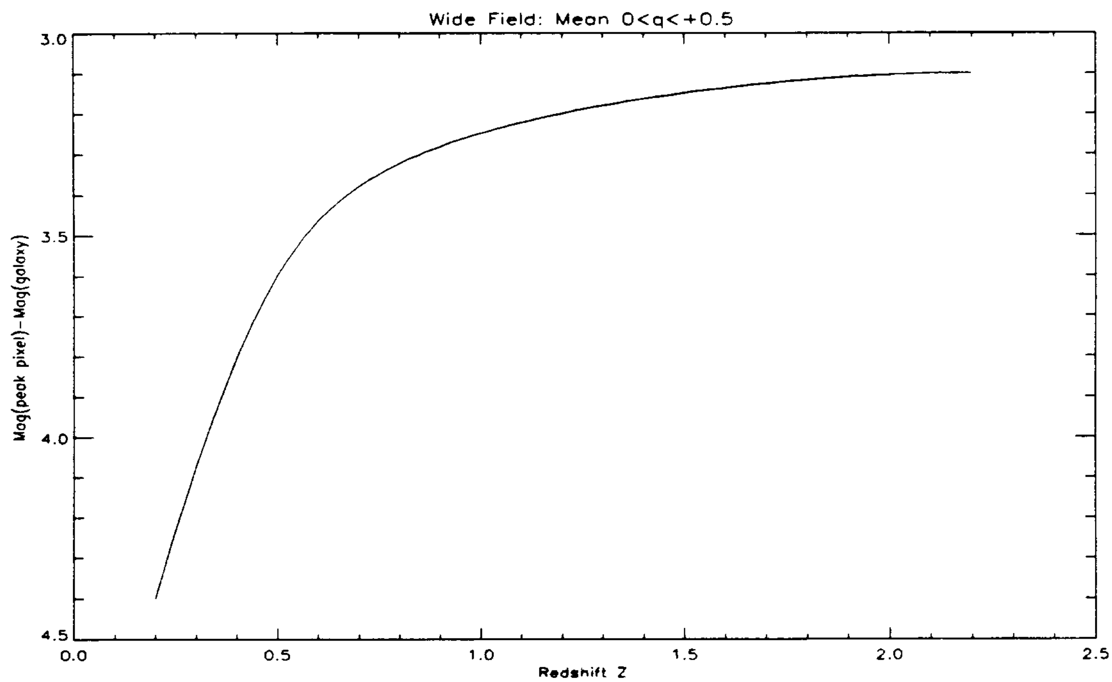

6.6 Exposure Time Estimation

In many instances one desires a certain SNR, and wishes to solve for the corresponding exposure time. Given the SNR, Equations 6.6, 6.7, or 6.14 can be solved for the exposure time, *t*. Since there are time-dependent and time-independent noise sources, quadratic equations are obtained. For example, we may solve equation 6.6 for the point source exposure time:

$$t = \frac{1}{2Y} \cdot (b + \sqrt{b^2 + 4aY})$$

where the term *A* contains the time-independent noise sources

$$a = \frac{readnoise^2 + 46P_{dark}}{sharpness}$$

and *B* contains the time-dependent noise sources

$$b = \frac{P_{dark} + P_{sky} + P_{background}}{sharpness} + R_{object}$$

and

$$Y = \left(\frac{R_{object}}{SNR}\right)^2$$

Equations for aperture photometry (6.7) and extended sources (6.12) can be solved with similar results. Parameters are as described in Tables 6.6, 6.8, and 6.9. We again note that the on-line WFPC2 Exposure Time Calculator program provides an easy method for these calculations.

6.7 Sample SNR Calculations

Below we give further examples of SNR calculations. The Appendix also gives tables of SNR values for a wide range of representative cases.

6.7.1 Point Sources

Simple Star, Manual Calculation, PSF Fitting

We begin with the simple example of V=20 star of spectral class G0. We want to observe with the PC using filter F555W. The star is somewhere near the ecliptic pole. We want to know the SNR for a 1200s CR-SPLIT exposure. Default ATD-GAIN=7 is used. We plan to use PSF fitting to analyze the data.

First we estimate the count rate for our target. Consulting Equation 6.2, Table 6.1, and Table 6.2 we have:

$$R_{object} = 2.5 \times 10^{11} \cdot \left[\int Q(\lambda)T(\lambda)d\lambda/\lambda\right] \cdot 10^{-0.4(V + AB_{\nu})}$$

$$= 2.5 \times 10^{11} \cdot [0.027] \cdot 10^{-0.4(20 + 0.02)} = 66$$

in units of $e^- s^{-1}$. Next we fill out Equation 6.6. To keep things simple we just use values from Table 6.6, and get the sky count rate from Table 6.4. There is no background light (i.e. no superposed galaxy), so $P_{background}$=0. The exposure time t=600 for each exposure of the CR-SPLIT:

$$SNR = \frac{R_{object} \cdot t}{\sqrt{R_{object} \cdot t + \frac{readnoise^2 + P_{dark} \cdot (t+46) + P_{sky} \cdot t + P_{background} \cdot t}{sharpness}}}$$

$$= \frac{66 \cdot 600}{\sqrt{66 \cdot 600 + \frac{(5.3)^2 + 0.004 \cdot (600+46) + (0.01 \cdot 600) + (0 \cdot 600)}{0.06}}}$$

$$= \frac{39600}{\sqrt{39600 + 611}} = 197$$

The SNR for the total 1200s exposure, i.e. both halves of the CR-SPLIT, would simply be:

$$SNR_{total} = SNR \cdot \sqrt{N} = 197 \cdot \sqrt{2} = 279$$

At these high SNR levels, it is likely that flat fielding would limit the photometric accuracy, rather than the noise. If we have a look at the terms in the SNR equation, we can see that the Poisson noise dominates; the term containing the sharpness and background noise sources is unimportant.

Just for fun, let us see what happens if we keep everything the same, but give the target V=25. Now we have R_{object}=0.66 e^{-} s^{-1}, and:

$$SNR = \frac{0.66 \cdot 600}{\sqrt{0.66 \cdot 600 + \frac{(5.3)^2 + 0.004 \cdot (600+46) + (0.01 \cdot 600) + (0 \cdot 600)}{0.06}}}$$

$$= \frac{396}{\sqrt{396 + 611}} = 12.5$$

We see that now the term with the background noise (in particular, the read noise) limits the SNR. For the full 1200s exposure the SNR_{total}=17.6.

Simple Star, Manual Calculation, Aperture Photometry

What if we now want to observe this same V=25 star, but we plan to reduce the data by measuring counts in a 0.5″ radius aperture? We now use Equation 6.7

instead, consult Table 6.7 for the encircled energy *f(r),* and note that 0.5″ corresponds to *r*=11.6 PC pixels:

$$SNR = \frac{f(r) \cdot R_{object} \cdot t}{\sqrt{(f(r) \cdot R_{object} \cdot t) + [readnoise^2 + P_{dark} \cdot (t+46) + P_{sky} \cdot t + P_{background} \cdot t] \cdot \pi r^2}}$$

$$= \frac{0.96 \cdot 0.66 \cdot 600}{\sqrt{(0.96 \cdot 0.66 \cdot 600) + ((5.3)^2 + 0.004(600+46) + 0.01 \cdot 600 + 0 \cdot 600) \cdot \pi (11.6)^2}}$$

$$= \frac{380}{\sqrt{380 + 15500}} = 3.0$$

Apparently using aperture photometry with a 0.5″ radius aperture reduces the SNR by a factor ~4 as compared to PSF fitting, for this background limited case.

Simple Star, SNR Tables, PSF Fitting

We now repeat the first calculation above for the V=20 star using the SNR tables in Appendix B. We look up the G0 spectral class and F555W filter (5500Å) in Table B.1, and obtain AB_V=0.02. For the V=20 star, we thus have V+AB_V=20.02. We look at Figure B.10 on page 234 and find this value on the horizontal axis. We locate exposure time 600s (one-half of the total 1200s CR-SPLIT exposure), and find SNR~200. For the total 1200s exposure the SNR would be $200\sqrt{2} = 280$.

Simple Star, On-Line Calculator, PSF Fitting

The above calculation for a V=20 GO star may also be performed using the WFPC2 Exposure Time Calculator program, which is available on the WFPC2 WWW pages at:

`http://www.stsci.edu/ftp/instrument_news/WFPC2/wfpc2_top.html`

To use this program, access the above address with NCSA Mosaic, Netscape, or a similar program. Once in the WFPC2 area, select the “Software Tools” page, and then the “ETC” page. For the first example above, choose the “Point Source” form and complete it as shown in Figure 6.2 for the 600s sub-exposure. Then clicks the “calculate” button and after a few seconds the result is displayed (Figure 6.3). The answer, SNR=198, is comparable to that obtained by the manual calculation above for the 600s sub-exposure (SNR=197). Alternatively, one can input the total exposure time (1200s), and then use the result farther down the output page for “No. Sub-Exposures = 2” (see Figure 6.4), thereby obtaining SNR=277 for the total 1200s CR-SPLIT exposure.

Figure 6.2: Sample Fill-out Form for WFPC2 On-Line Exposure Time Calculator.

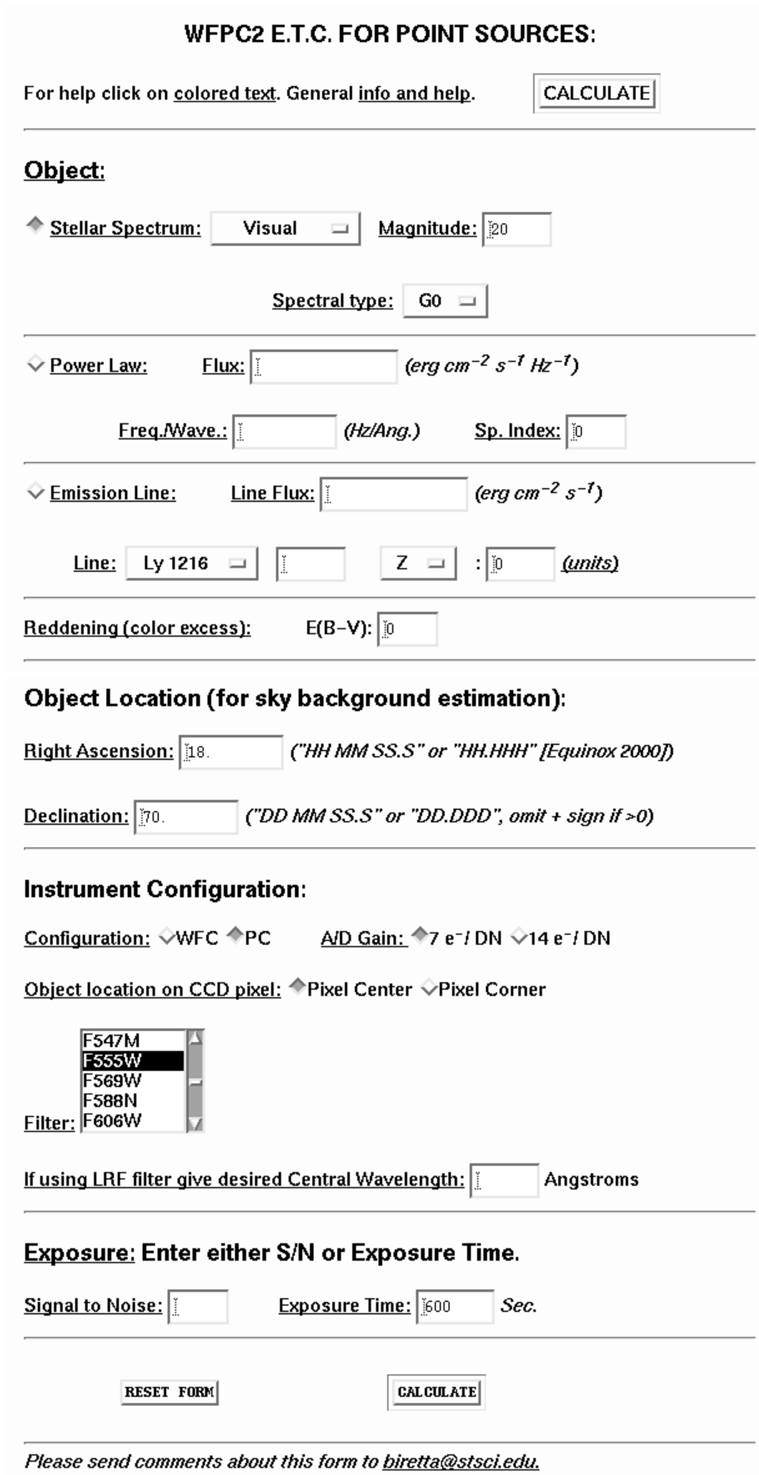

WFPC2 E.T.C. FOR POINT SOURCES:

For help click on colored text. General info and help. CALCULATE

Object:

Stellar Spectrum: Visual Magnitude: 20

Spectral type: G0

Power Law: Flux: (erg cm^{-2} s^{-1} Hz^{-1})

Freq./Wave.: (Hz/Ang.) Sp. Index: 0

Emission Line: Line Flux: (erg cm^{-2} s^{-1})

Line: Ly 1216 Z : 0 (units)

Reddening (color excess): E(B−V): 0

Object Location (for sky background estimation):

Right Ascension: 18. ("HH MM SS.S" or "HH.HHH" [Equinox 2000])

Declination: 70. ("DD MM SS.S" or "DD.DDD", omit + sign if >0)

Instrument Configuration:

Configuration: WFC PC A/D Gain: 7 e⁻/ DN 14 e⁻/ DN

Object location on CCD pixel: Pixel Center Pixel Corner

Filter: F547M F555W F569W F588N F606W

If using LRF filter give desired Central Wavelength: Angstroms

Exposure: Enter either S/N or Exposure Time.

Signal to Noise: Exposure Time: 600 Sec.

RESET FORM CALCULATE

Please send comments about this form to biretta@stsci.edu.

Figure 6.3: Sample Results from WFPC2 On-Line Exposure Time Calculator.

WFPC2 ETC results

Final Result

Signal-to-Noise Ratio = 198.1

Exposure Time Quantization

Figure 6.4: Sample Results on CR-SPLITing from WFPC2 On-Line Exposure Time Calculator Results Page.

No. Sub-Exposures	Total SNR	Pixels Lost
(No Split)	280.8	3.981250%
2	277.4	0.039626%
3	277.7	0.000234%
4	277.6	0.000001%
6	276.8	0.000000%
8	275.8	0.000000%
12	273.6	0.000000%
16	271.4	0.000000%
32	262.8	0.000000%

Star Superposed on Galaxy, Manual Calculation

We now consider a B=25 point source of spectral class B0, which is superposed on an elliptical galaxy with σ_V=22 mag arcsecond^{-2}. We want to compute the SNR obtained from a one-orbit (40 min.) non-CR-SPLIT observation in filter F300W on the WFC. PSF fitting will be used for the photometry.

We begin by computing the total count rate for the target. Using Table 6.2 we see that this target will have V=25.31. From Table 6.1 we obtain the filter efficiency and mean wavelength. Interpolating by mean wavelength in Table 6.2 we obtain AB_V=-0.83 for the B0 star. Using Equation 6.2 we have:

$$R_{object} = 2.5 \times 10^{11} \cdot \left[\int Q(\lambda) T(\lambda) d\lambda / \lambda\right] \cdot 10^{-0.4(V + AB_V)}$$

$$= 2.5 \times 10^{11} \cdot [0.00519] \cdot 10^{-0.4(25.31 - 0.83)} = 0.21$$

in units of $e^{-}\ s^{-1}$. Next we consider the background light from the superposed galaxy. We set σ_V=22 mag arcsecond^{-2} in Equation 6.11, and AB_ν=3.63 for a gE galaxy at λ=3000Å (filter F300W) from Table 6.2. Hence the count rate per pixel due to the background light is:

$$P_{background} = 2.5\times10^{11}\cdot\left[\int Q(\lambda)T(\lambda)d\lambda/\lambda\right]\cdot 10^{-0.4(\sigma_V + AB_\nu + 5)}$$

$$= 2.5\times10^{11}\cdot[0.00519]\cdot 10^{-0.4(22+3.63+5)} = 0.00073$$

For the sky background, we note that Table 6.4 has no entry for F300W, so that the sky must be unimportant. If we wanted to calculate it anyway, as a check, we would use Table 6.3 for the sky brightness, Table 6.2 for the sky's AB_ν, and again Equation 6.11. We will assume the target is near the ecliptic pole.

$$P_{sky} = 2.5\times10^{11}\cdot\left[\int Q(\lambda)T(\lambda)d\lambda/\lambda\right]\cdot 10^{-0.4(\sigma_V + AB_\nu + 5)}$$

$$= 2.5\times10^{11}\cdot[0.00519]\cdot 10^{-0.4(23.3+3.12+5)} = 0.00035$$

For the sharpness function we will use "pixel corner" values (least optimistic choice) from Table 6.5. Using read noise and dark current from Table 6.6, and Equation 6.6 for point source SNR:

$$SNR = \frac{R_{object}\cdot t}{\sqrt{R_{object}\cdot t + \dfrac{readnoise^2 + P_{dark}\cdot(t+46) + P_{sky}\cdot t + P_{background}\cdot t}{sharpness}}}$$

$$= \frac{0.21\cdot 2400}{\sqrt{0.21\cdot 2400 + \dfrac{(5.3)^2 + 0.004\cdot(2400+46) + (0.00035\cdot 2400) + (0.00073\cdot 2400)}{0.103}}}$$

$$= \frac{504}{\sqrt{504+393}} = 16.8$$

for this single exposure. The SNR for multiple 40 min. exposures would be simply $16.8(N^{1/2})$, where N is the number of exposures.

Star Superposed on Galaxy, On-Line Calculator

The above calculation could also be performed with the on-line WFPC2 Exposure Time Calculator. One would select the "Point source + stellar background” form, and complete it as in Figure 6.5, and then click on “calculate.” Figure 6.6 shows some of the results.

6.7.2 Extended Sources

In general, the signal-to-noise level for extended sources can be computed by comparing the expected signal, S, in each pixel, determined from Equations 6.8 through 6.13, to the noise $N=(S+B)^{1/2}$, where B is the equivalent background, determined in a manner similar to that for point sources. Unlike for point sources, the calculation does not, in a first approximation, involve the sharpness of the point spread function. For example, let us consider the observation of a source with a V surface brightness of 24 mag arcsec^{-2}, assuming the F569W filter F569W, WFC camera, and sky background V=23.3 mag arcsec^{-2}. The signal-to-noise estimate goes as follows. The signal in each WFC pixel is 24.0+5.0 = 29.0 magnitude. By Equation 6.11, the total signal collected from the source in a 3000 second integration is S = 41.8 electrons, neglecting the small AB color correction. The sky signal per pixel is 76.8 electrons. The dark current is ~12 electrons. The total equivalent background is thus $B = 76.8+5.3^2+12 = 116.9$ electrons, larger than the signal detected, thus the noise is background-dominated. The noise is $N=(S+B)^{1/2}$= 12.6 electrons, and the signal-to-noise *per pixel* expected in this case is 3.3. Similar calculations can be carried out for other filters; for observations in narrow-band filters and in the UV, the sky background signal will usually be unimportant. For very long observations of faint objects, other noise terms, such as flat field uncertainty, and errors in dark (and possibly bias) subtraction, must be considered more carefully.

If the scale of features in the target is larger than one pixel, the signal-to-noise can sometimes be improved by smoothing the observed image or - if read noise is a significant contributor - by reading the image out in AREA mode (see section 2.8, “CCD Orientation and Readout”, on page 31).

6.7.3 Emission Line Sources

The signal-to-noise ratio calculation for point-like or extended emission-line sources is similar to that for continuum sources. However, the details of the calculation are different, because of the units used for the line flux, and because the flux is in a narrow line. The integrated filter efficiency is not relevant for the signal calculation; what matters is the total system throughput QT at the wavelength of the line, which can be determined from inspection of the Figures in section A.2, “Passbands including the System Response”, on page 211. For lines near the center of the filter bandpasses the QT_{max} values from Table 6.1 can be used. The total signal expected for a point source of line strength F, expressed in erg s^{-1} cm^{-2}, is $S=2.28\text{x}10^{12}\ \lambda\ t\ QT\ F$, where t is the exposure time in seconds, and λ the wavelength of the line in Angstroms. Thus, H_{α} emission at 6563Å, with flux $F=10^{-16}$ erg s^{-1} cm^{-2}, observed for 1000 seconds through the F656N filter (total system throughput QT=0.104 from “F656N, F658N, F673N, F675W, F702W, F785LP” on page 217), will produce a total signal of S=155 electrons. The equivalent background per pixel is read-noise dominated: $B=1+5.3^2+4=33$, for a

Figure 6.5: Point Source + Stellar Background Fill-out Form for WFPC2 On-Line Exposure Time Calculator. SNR is calculated for B=25 star (class B0) superposed on an elliptical galaxy (gE) with σ_V=22. WFC is used with F300W.

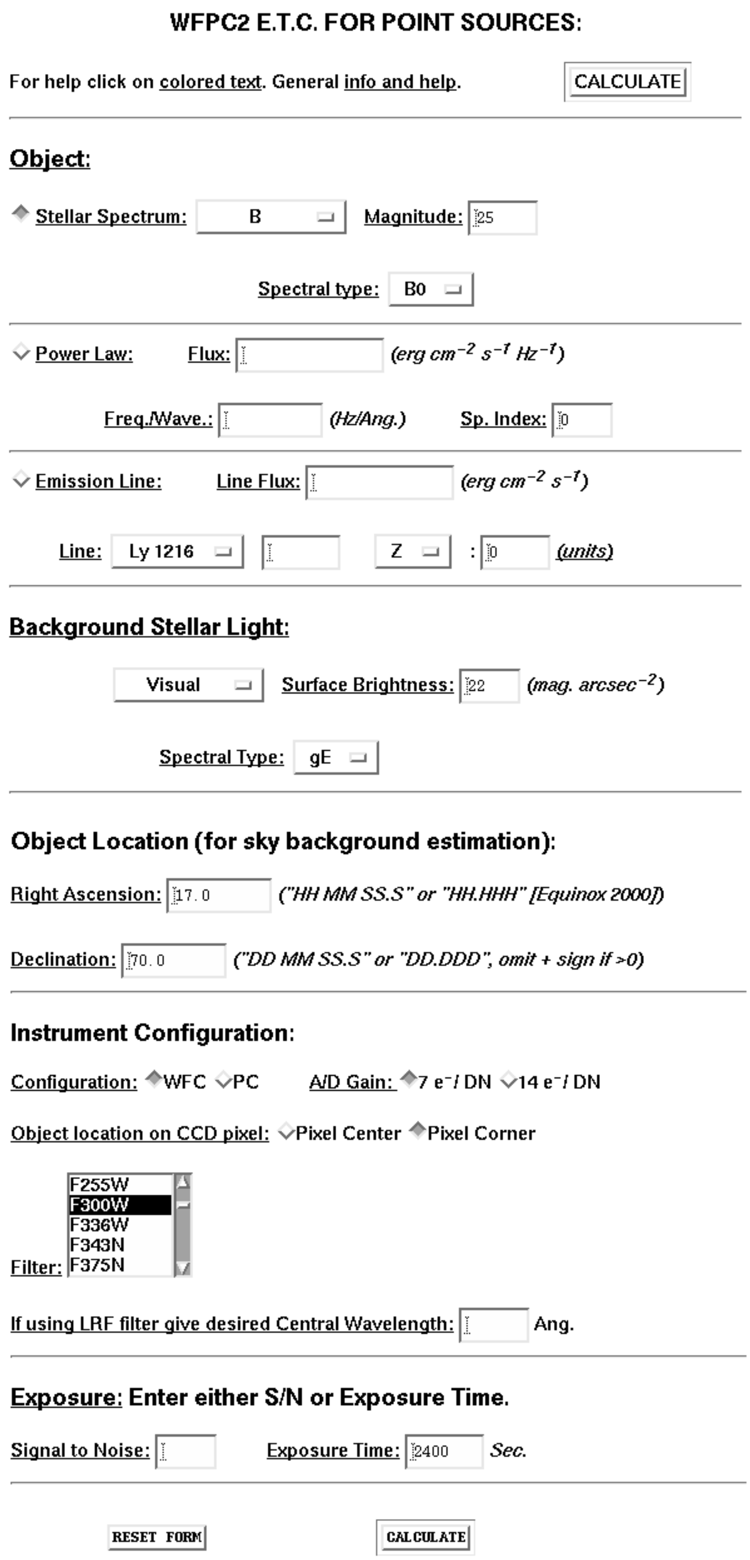
WFPC2 E.T.C. FOR POINT SOURCES:

For help click on colored text. General info and help. CALCULATE

Object:

Stellar Spectrum: B Magnitude: 25

Spectral type: B0

Power Law: Flux: (erg cm^{-2} s^{-1} Hz^{-1})

Freq./Wave.: (Hz/Ang.) Sp. Index: 0

Emission Line: Line Flux: (erg cm^{-2} s^{-1})

Line: Ly 1216 Z : 0 (units)

Background Stellar Light:

Visual Surface Brightness: 22 (mag. $arcsec^{-2}$)

Spectral Type: gE

Object Location (for sky background estimation):

Right Ascension: 17.0 ("HH MM SS.S" or "HH.HHH" [Equinox 2000])

Declination: 70.0 ("DD MM SS.S" or "DD.DDD", omit + sign if >0)

Instrument Configuration:

Configuration: WFC PC A/D Gain: 7 e⁻/ DN 14 e⁻/ DN

Object location on CCD pixel: Pixel Center Pixel Corner

Filter: F255W F300W F336W F343N F375N

If using LRF filter give desired Central Wavelength: Ang.

Exposure: Enter either S/N or Exposure Time.

Signal to Noise: Exposure Time: 2400 Sec.

RESET FORM CALCULATE

Figure 6.6: Sample Output from WFPC2 On-Line Exposure Time Calculator.

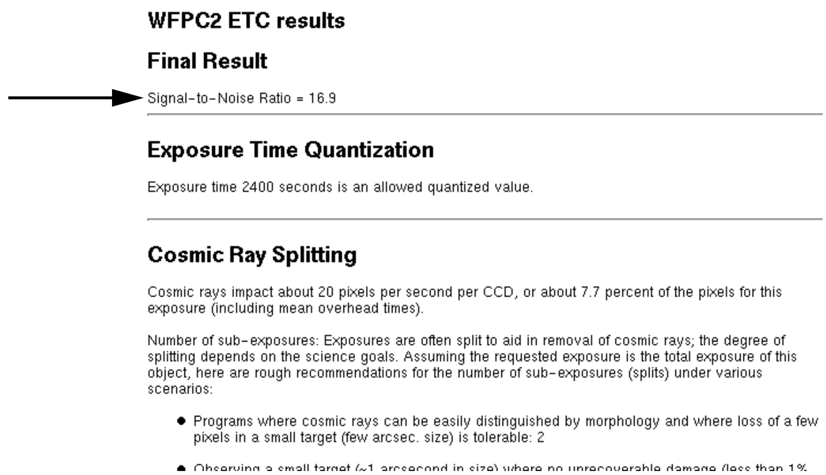
WFPC2 ETC results

Final Result

Signal-to-Noise Ratio = 16.9

Exposure Time Quantization

Exposure time 2400 seconds is an allowed quantized value.

Cosmic Ray Splitting

Cosmic rays impact about 20 pixels per second per CCD, or about 7.7 percent of the pixels for this exposure (including mean overhead times).

Number of sub-exposures: Exposures are often split to aid in removal of cosmic rays; the degree of splitting depends on the science goals. Assuming the requested exposure is the total exposure of this object, here are rough recommendations for the number of sub-exposures (splits) under various scenarios:

- Programs where cosmic rays can be easily distinguished by morphology and where loss of a few pixels in a small target (few arcsec. size) is tolerable: 2
- Observing a small target (~1 arcsecond in size) where no unrecoverable damage (less than 1%

background noise of ~6 electrons. The total noise is dominated by photon noise from the signal itself, and the signal-to-noise ratio achieved in this observation is over 10.

If the source is extended, the expected signal *per arcsecond* must be multiplied by the effective pixel area: 0.0099 arcsec^2 for the WF, 0.0021 for the PC. For a line flux of, say, F = 10^{-15} erg s^{-1} cm^{-2} arcsec^{-2}, this corresponds to 15 electrons in 1000 seconds for a WFC pixel. The noise is now dominated by the background, and the single-pixel signal-to-noise ratio is $15/(33 + 15)^{1/2} \sim 2.1$.

Extended Line Emission Source, Manual Calculation

We now consider a detailed example of a planetary nebula observed on the PC with the F502N filter. The nebula has a diameter of 5″ and a total flux F=4x10^{-13} erg s^{-1} cm^{-2} in the [OIII] 5007Å line. We want to estimate the SNR for an 1800s exposure, which will be CR-SPLIT.

First we must estimate the flux per square arcsecond. Using the nebula diameter, the average brightness is I_ν = 2.0x10^{-14} erg s^{-1} cm^{-2} arcsec^{-2}. From the plots in section A.2, “Passbands including the System Response”, on page 211, we see that QT=0.053. Using Equation 6.10 for the target count rate per pixel:

$$P_{object} = 4.8 \times 10^9 \cdot (QT) \cdot I_\nu \cdot \lambda$$

$$= 4.8 \times 10^9 \cdot (0.053) \cdot 2.0 \times 10^{-14} \cdot 5007 = 0.025$$

Next we estimate the SNR for each 900s sub-exposure using Equation 6.14 and Table 6.9. For this narrow filter the sky background can be ignored. We presume there is no background light from astrophysical sources:

$$SNR = \frac{P_{object} \cdot t}{\sqrt{P_{object} \cdot t + (readnoise^2 + P_{dark} \cdot (t+46) + P_{sky} \cdot t + P_{background} \cdot t)}}$$

$$= \frac{0.025 \cdot 900}{\sqrt{0.025 \cdot 900 + (5.3^2 + 0.004 \cdot (900+46) + 0 \cdot 900 + 0 \cdot 900)}} = 3.1$$

Hence SNR=3.1 per pixel for each 900s sub-exposure. The SNR per pixel for the total 1800s is

$$SNR_{total} = SNR\sqrt{N} = 3.1 \cdot \sqrt{2} = 4.3$$

The SNR for the entire nebula is this SNR per pixel times the square root of the number of pixels in the image, or ~420. In actuality, uncertainties in the photometric calibration and flat fields, would limit the SNR to ~100.

Extended Line Emission Source, On-Line Calculator

The above example could be calculated with the “Extended Source” form of the ETC program. The fill-out form would be completed as shown in Figure 6.7. We have selected “[OIII] 5007” on the emission line menu, and have left the redshift (z) set to zero. The PC and F502N filter are selected. Note we have entered the exposure time as 1800s. Scrolling down through the output page we find a table of SNR for various CR-SPLITings of the exposure (See Figure 6.8). “No. Sub-Exposures = 2” gives the answer we want, SNR=4.5 per pixel.

Figure 6.7: Extended Source Form for WFPC2 On-Line Exposure Time Calculator. Here target is galactic [OIII] 5007 line emission source and is observed on PC with filter F502N. SNR is computed for 1800s exposure.

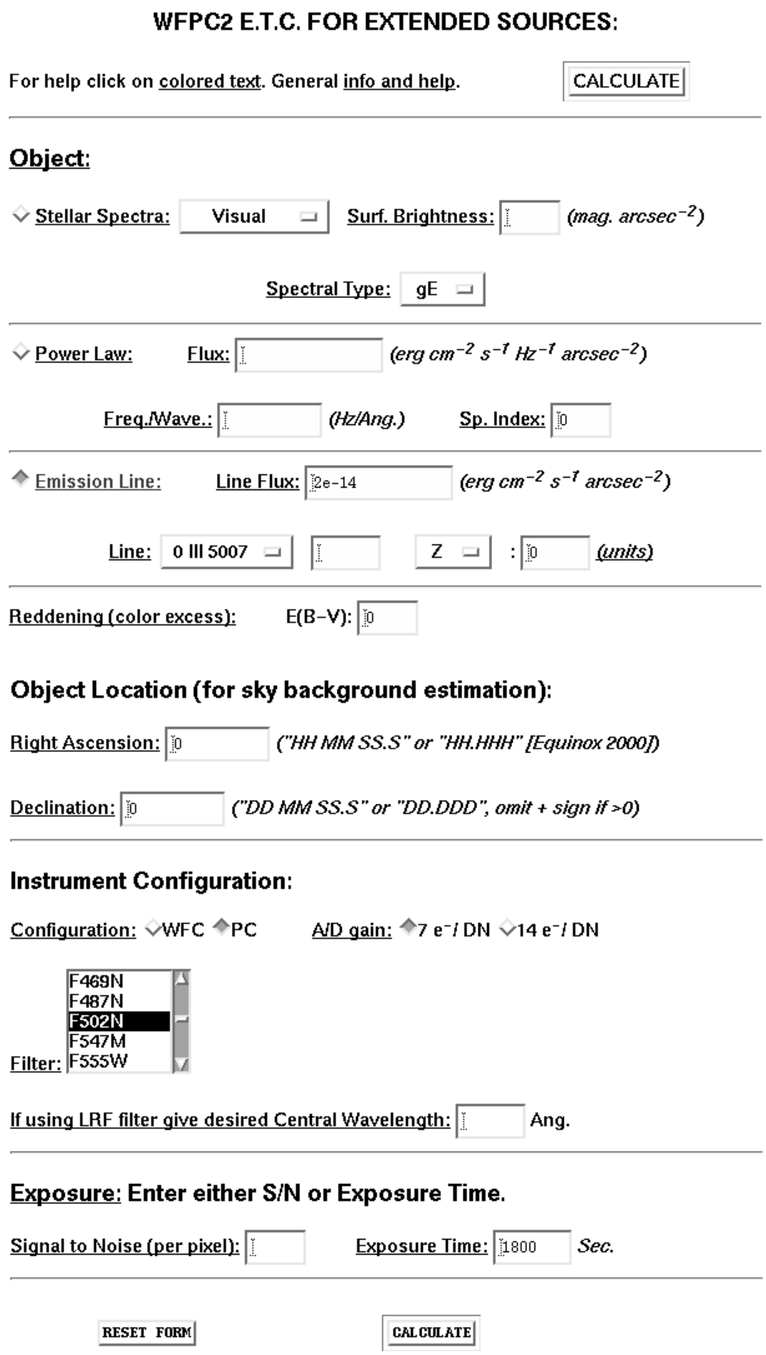

Figure 6.8: Sample Output from WFPC2 On-Line Exposure Time Calculator.

No. Sub-Exposures	Total SNR	Pixels Lost
(No Split)	5.3	5.856250%
2	4.5	0.085739%
3	4.1	0.000744%
4	3.8	0.000005%
6	3.3	0.000000%
8	2.9	0.000000%
12	2.5	0.000000%
16	2.2	0.000000%
32	1.6	0.000000%

Line Emission Point Source w/ LRF, Manual Calculation

In this example we consider an unresolved source of H_{α} emission in a galaxy at redshift z=0.22 with flux F=1.5x10^{-16} erg s^{-1} cm^{-2}. We want the SNR for a 2400s exposure without CR-SPLITing.

Since the redshift is significant, we cannot observe with the F656N filter. Instead we will use the Linear Ramp Filter (LRF). The observed wavelength will be 8007Å. From Table 3.7 on page 48 we see that this will be observed using the FR868N filter on CCD WF3. Combining the LRF transmission from Figure 3.2 and the "WFPC2 + OTA System Throughput" from Figure 2.4 we estimate QT=0.054. We compute the count rate using Equation 6.4: To estimate the SNR

$$R_{object} = 2.3 \times 10^{12} \cdot (QT) \cdot F \cdot \lambda$$

$$= 2.3 \times 10^{12} \cdot (0.054) \cdot (1.5 \times 10^{-16}) \cdot 8007 = 0.15$$

we use Equation 6.6, which assumes that PSF fitting will be used to analyze the image. Since the filter is narrow, we will ignore the sky emission. We use Table 6.6 for the WFC sharpness and also the read noise.

$$SNR = \frac{R_{object} \cdot t}{\sqrt{R_{object} \cdot t + \dfrac{readnoise^2 + P_{dark} \cdot (t + 46) + P_{sky} \cdot t + P_{background} \cdot t}{sharpness}}}$$

$$= \frac{0.15 \cdot 2400}{\sqrt{0.15 \cdot 2400 + \dfrac{5.3^2 + 0.004(2400 + 46) + 0 \cdot 2400 + 0 \cdot 2400}{0.11}}}$$

$$= \frac{360}{\sqrt{360 + 344}} = 14$$

which is for an un-split 2400s exposure. The Poisson noise and background noises contribute nearly equally. For three such exposures over three orbits

$$SNR_{total} = SNR\sqrt{N} = 14\sqrt{3} = 23.$$

Line Emission Point Source w/ LRF, On-Line Calculator

The above calculation can be performed using the ETC program. The “Point Source” form is used. “Emission Line” source and the “H 6563” line are selected; the redshift is set to 0.22. The program will automatically choose between PC and WFC, depending on the LRF setting. The least optimistic case of placing the object on a “pixel corner” is selected. The filter “LRF” is selected from the filter menu, and 8007Å is given for the central wavelength. The exposure time is specified as 2400s. (See Figure 6.9 for example of completed form.) The result is SNR=13.1 for the un-split 2400s exposure (Figure 6.10), which is comparable to the manual calculation of SNR=14.

Figure 6.9: Point Source Form for WFPC2 On-Line Exposure Time Calculator. Target is unresolved galaxy (z=0.22) nucleus with Hα line emission which is observed with LRF. SNR is computed for 2400s exposure.

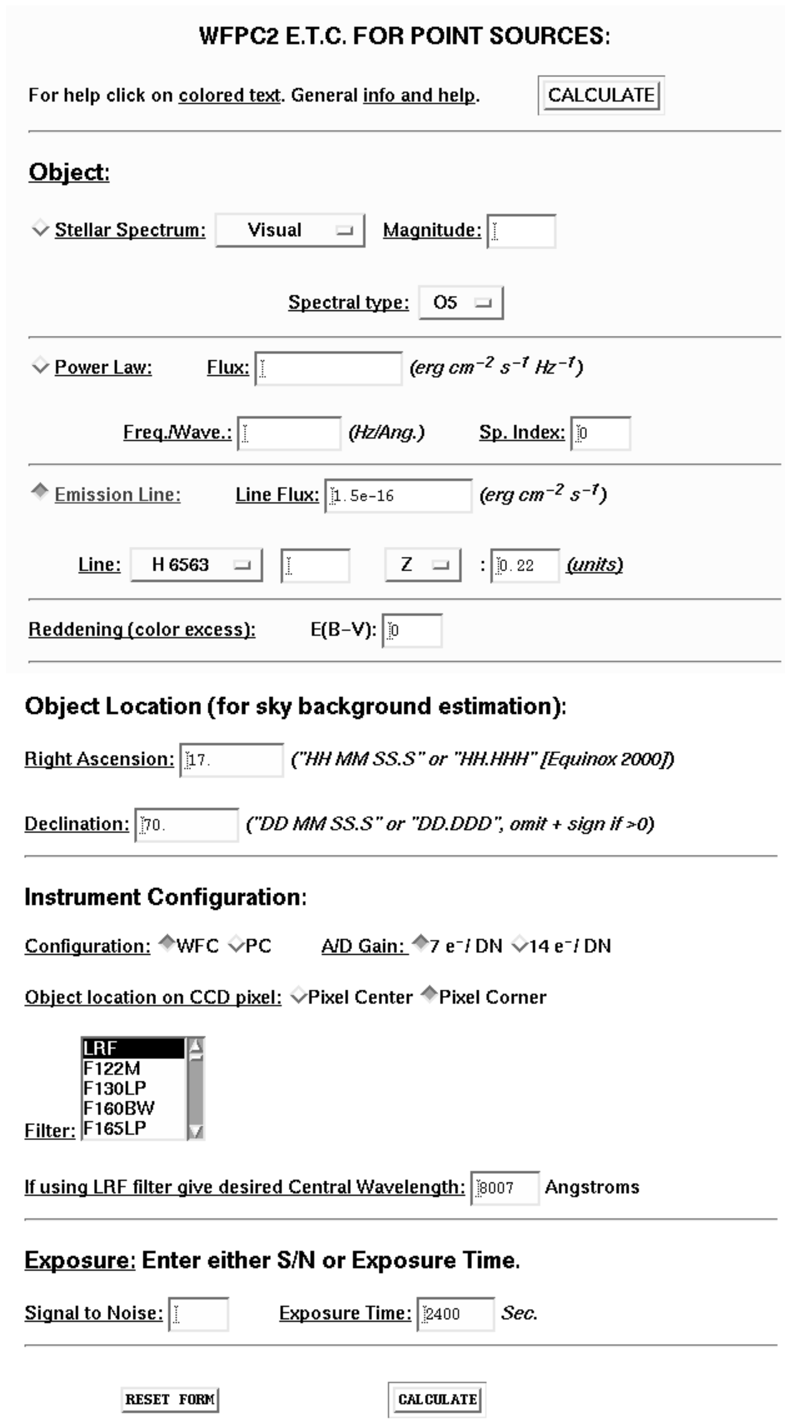

Figure 6.10: Sample Output for WFPC2 On-Line Exposure Time Calculator.

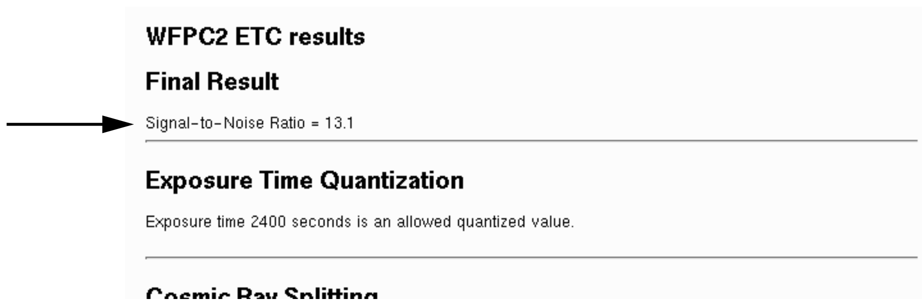

6.8 Red Leaks in UV Filters

The presence of significant red leaks in the UV filters, together with the much greater sensitivity and wavelength coverage in the red part of the spectrum, can make UV observation and calibration difficult. Observers must sometimes be prepared to take additional frames at red wavelengths, in order to estimate the contribution of red leak to the UV counts. The counts contributed by red leak can be a significant noise source, and must also be taken into account during SNR and exposure time estimation. See section 3.7 on page 57 for detailed information. Note that the SYNPHOT synthetic photometry package can be used to estimate counts due to red leak for particular filter / target combinations.

6.9 Time Dependence of UV Response

The UV throughput of the WFPC2 degrades in a predictable way after each monthly decontamination. The photometric calibration given in Section 6.1 is applicable at the start of each cycle, and measurements taken at other times must be corrected to account for the change in sensitivity since the last decontamination. In addition, a long-term change in sensitivity is present for the F160BW and F170W filter observations on the PC, and may be present to a lesser degree at other wavelengths.

Figure 6.11 shows the photometric monitoring data for the standard star GRW+70D5824 (a white dwarf classified DA3; B-V = -0.09) in the WF3 and PC1 for the set of filters which are routinely monitored. The dotted vertical lines mark the dates of the decontaminations. The solid vertical lines labeled “-88” mark the date the operating temperature was changed from -76˚C to -88˚C (April 24, 1994). The following information is for the period following the cooldown date. Figure 6.11 shows that the effect of contamination on the F675W and F814W filter observations is essentially negligible, but it rises toward the UV until it reaches values of 30% - 40% per month for the F160BW filter. Table 6.10 shows

Table 6.10: Change in WFPC2 Throughput Over 30 Days[a].

Filter	PC1	WF2	WF3	WF4
F160BW	-0.263 ± 0.030		-0.393 ± 0.051	
F170W	-0.160 ± 0.011	-0.284 ± 0.005	-0.285 ± 0.006	-0.232 ± 0.006
F218W	-0.138 ± 0.009		-0.255 ± 0.010	
F255W	-0.070 ± 0.007		-0.143 ± 0.009	
F336W	-0.016 ± 0.008 (-0.038 ± 0.018)	(-0.043 ± 0.010)	-0.057 ± 0.011 (-0.046 ± 0.008)	(-0.047 ± 0.007)
F439W	-0.002 ± 0.007 (0.002 ± 0.014)	(-0.022 ± 0.007)	-0.021 ± 0.010 (-0.023 ± 0.009)	(-0.023 ± 0.007)
F555W	-0.014 ± 0.006 (0.007 ± 0.013)	(-0.007 ± 0.007)	-0.016 ± 0.008 (-0.009 ± 0.009)	(-0.008 ± 0.008)
F675W	-0.001 ± 0.006 (-0.020 ± 0.020)	(0.001 ± 0.011)	-0.001 ± 0.006 (0.002 ± 0.011)	(0.004 ± 0.011)
F814W	0.007 ± 0.007 (0.013 ± 0.019)	(-0.002 ± 0.009)	0.003 ± 0.008 (-0.000 ± 0.009)	(-0.002 ± 0.010)

a. Values in parentheses are from the ω Cen observations.

the monthly decline in throughput based on this data. The values in parentheses are based on similar observations of the globular cluster ω Cen (NGC 5139; mean B-V ~ 0.7 mag). In general the values derived from the ω Cen data are in good agreement with the values derived from GRW+70D5824 data.

A slight difference between the throughput declines for GRW+70D5824 and ω Cen might be expected due to differences in spectral shape, especially for filters like F336W which have a substantial red leak. However, even in the case of F336W the effect should be less than 0.01 mag based on SYNPHOT simulations.

Figure 6.12 shows the throughput decline in all four chips as a function of days since the last decontamination for the F170W filter. The contamination rate is remarkably constant during each decontamination cycle, and can be accurately modeled by a simple linear decline in throughput following the decontaminations, which appear to return the throughput to roughly the nominal value each month. While the contamination rates are similar for the three WF chips, the values for the PC are much lower.

In addition to the monthly changes in throughput there is now evidence for a long-term variation in the F170W data on the PC, where the throughput has *increased* at the rate of 4.8% $\pm$ 0.3% per year. This is evident in Figure 6.11, but is much clearer in Figure 6.12 where the data before and after Jan. 1, 1995 are compared, and in Figure 6.13 where the effect of the monthly decontamination is removed. The F160BW filter shows an even stronger trend but with larger uncertainties (i.e., an increase of 9.0% $\pm$ 1.7% per year). The WF chips do NOT show this effect, nor do the observations on the PC at longer wavelengths. One possible explanation of the throughput increase is that WFPC2 was flown with some initial contaminant on the PC1 optics which is slowly evaporating on-orbit. The pre-launch thermal vacuum test gave evidence of elevated contamination in PC1, which is consistent with this hypothesis.

ISR 96-4 will describe detailed results of this monitoring (available from our WWW site). Observers are advised to consult the STScI WFPC2 WWW page for the latest information at the following address:

```
http://www.stsci.edu/ftp/instrument_news/WFPC2/wfpc2_top.html
```

Figure 6.11: Photometric Monitoring Data for WFPC2.

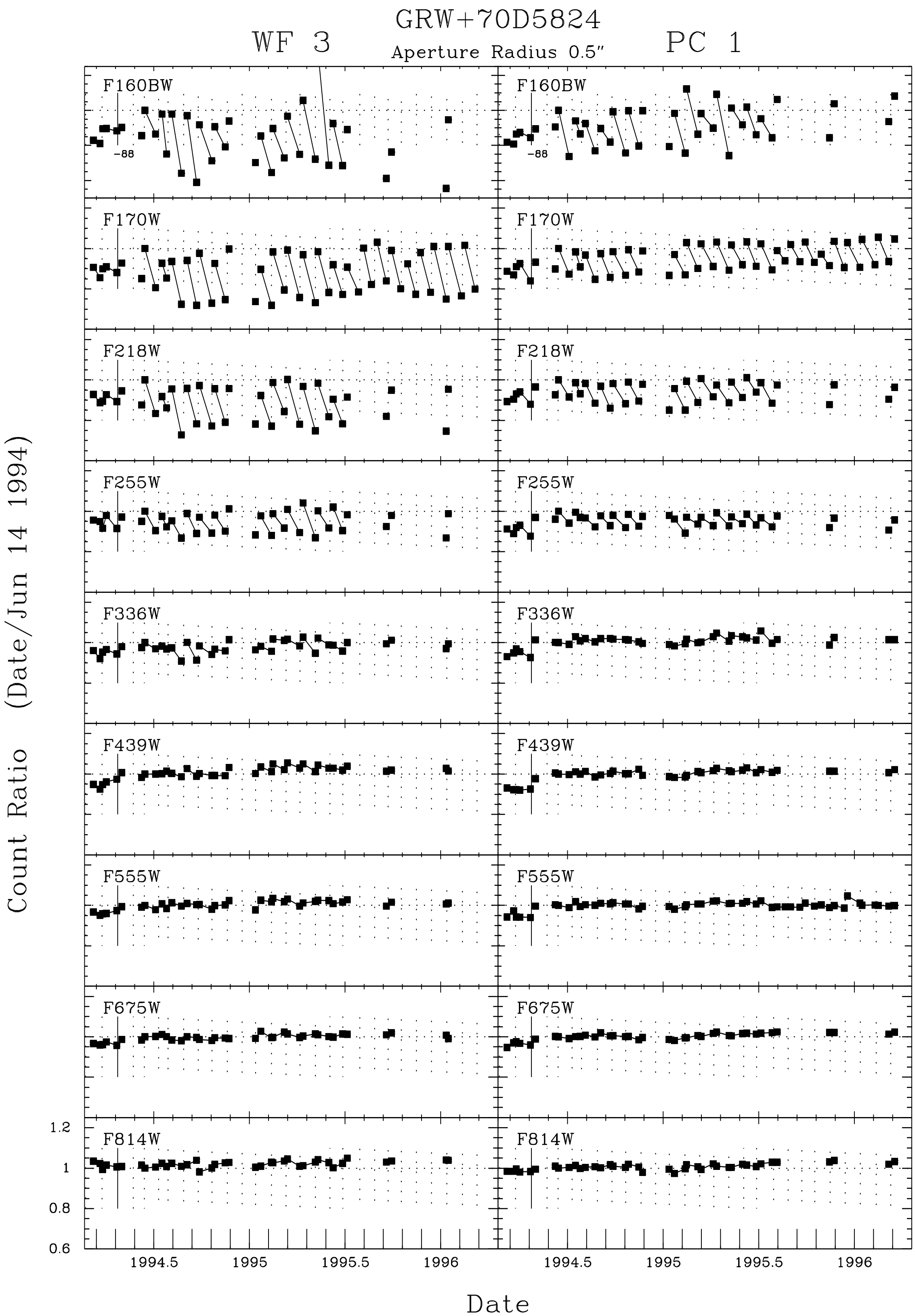

Figure 6.12: Throughput for the F170W Filter Following Decontaminations.

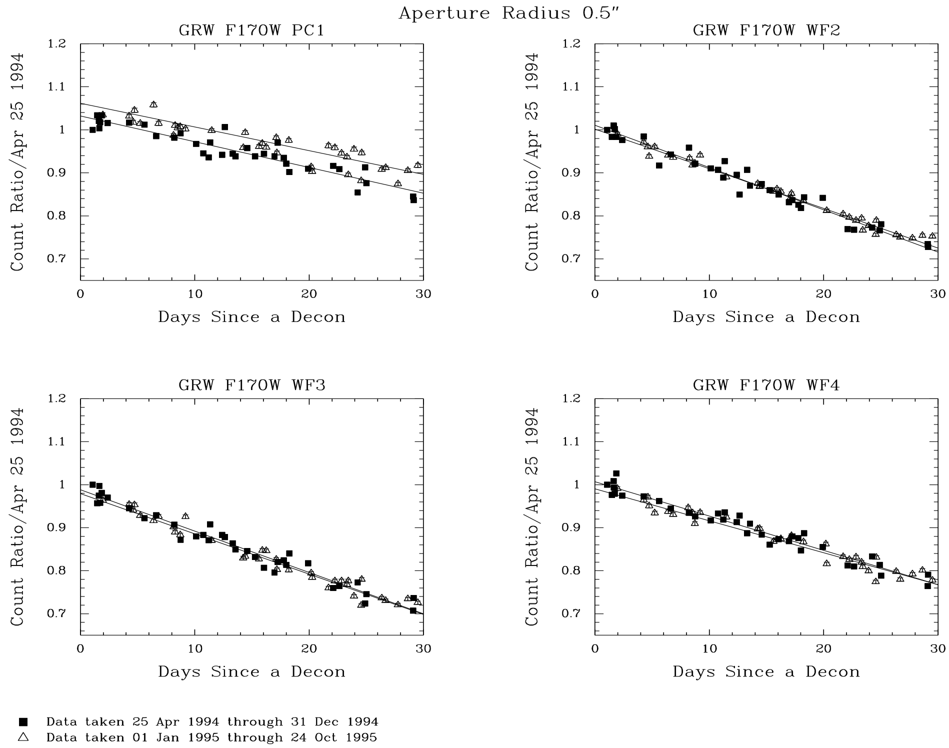

Figure 6.13: Change in Throughput vs. Time.[1]

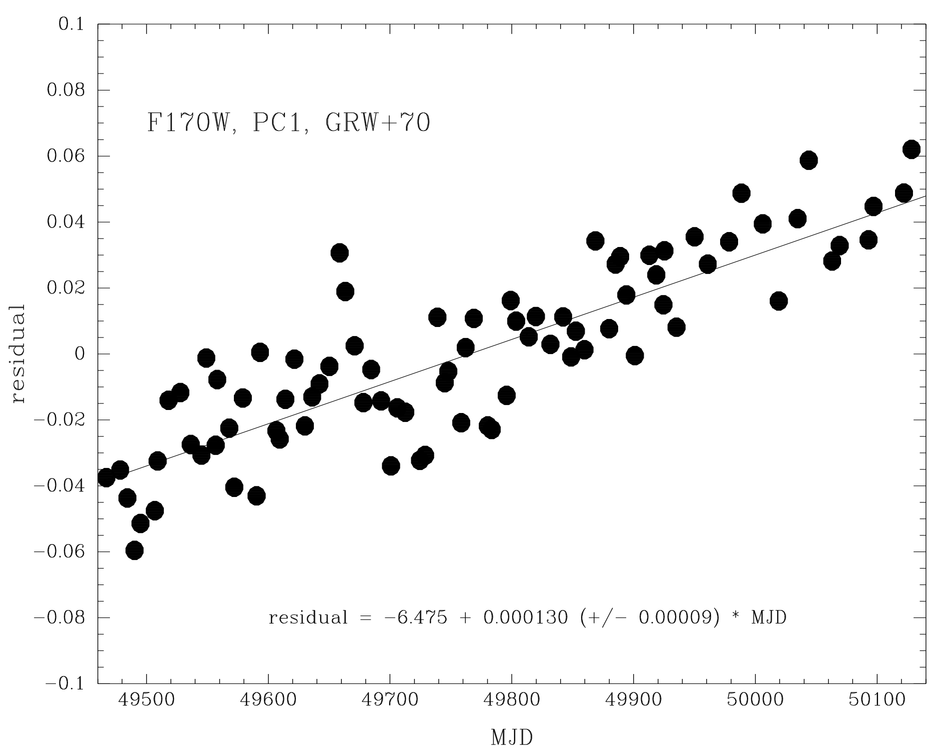

1. Determined after removing the effects of the monthly decontamination